Vol 14 No 11, November 2005
1009-1963/2005/14(11)/2246-05

Chinese Physics

© 2005 Chin. Phys. Soc.
and IOP Publishing Ltd

Host dependent thermal stability and frequency upconversion of Er^{3+}-doped heavy metal oxyfluoride germanate glasses*

Xu Shi-Qing(徐时清)[a)b)c)†], Fang Da-Wei(方达伟)[a)], Zhang Zai-Xuan(张在宣)[a)],
Zhao Shi-Long(赵士龙)[a)], Zhang Li-Yan(张丽艳)[a)],
Wang Bao-Ling(王宝玲)[a)], and Jiang Zhong-Hong(姜中宏)[b)]

[a)] *College of Information Engineering, China Jiliang University, Hangzhou* 310018, *China*
[b)] *Shanghai Institute of Optics and Fine Mechanics, Chinese Academy of Sciences, Shanghai* 201800, *China*
[c)] *Graduate School of Chinese Academy of Sciences, Beijing* 100039, *China*

(Received 19 December 2004; revised manuscript received 16 July 2005)

The upconversion properties of Er^{3+}-doped heavy metal oxyfluoride germanate glasses under 975 nm excitation have been investigated. The intense green (551 and 529 nm) and relatively weak red (657 nm) emissions corresponding to the transitions $^4S_{3/2} \rightarrow {}^4I_{15/2}$, $^2H_{11/2} \rightarrow {}^4I_{15/2}$ and $^4F_{9/2} \rightarrow {}^4I_{15/2}$, respectively, were simultaneously observed at room temperature. The content of PbF_2 has an important influence on the upconversion luminescence emission. With increasing content of PbF_2, the intensities of green (529 nm) and red (657 nm) emissions increase slightly, while the green emission (551 nm) increases markedly. These results suggest that PbF_2 has an influence on the green (551 nm) emission more than on the green (529 nm) and red (657 nm) emissions.

Keywords: optical materials, glass, Raman spectroscopy, optical properties, infrared spectroscopy
PACC: 4280S, 3350D, 2320C

1. Introduction

Solid-state blue and green light sources are desirable for high-density optical storage, colour displays, optoelectronics, and medical diagnostics.[1−3] Er^{3+} is one of the most extensively studied rare-earth ions for green laser operation based upon upconversion.[4,5] The host materials for Er^{3+}-doping are very important for obtaining high efficient upconversion signal. Because host materials with low phonon energy can reduce the non-radiative loss due to the mutiphonon relaxation and thus realize strong upconversion luminescence. For various glass hosts, the conventional oxide glasses, such as silicate, phosphate, and borate glasses, are difficult to produce strong upconversion emission due to their high phonon energies.[6] Though fluoride glasses have been extensively studied due to their low phonon energies, oxide glasses are more appropriate in practical applications for their high chemical and thermal stability.[7] Compared with other oxide glasses, heavy metal glasses and germanate glasses (which have lower phonon energies in the oxide glasses) may be better hosts because of high resistance combined with high refractive index, which enhances radiative transitions of Er^{3+}.[8,9] Although upconversion luminescence has been reported in Er^{3+}-doped germanate glasses,[10,11] it is weak. Efforts to enhance upconversion luminescence of Er^{3+}-doped germanate glasses are still attracting the attention of researchers.

As is known, glasses based on mixed oxide-fluoride systems combine the good optical properties of halide glasses (a broad range of optical transmittance and low optical losses) with the better chemical and thermal stability of oxide glasses.[12] In this paper, Er^{3+}-doped new heavy metal oxyfluoride germanate glasses suitable for making upconversion optical devices have been fabricated. Intense upconversion luminescence is observed, and the influence of PbF_2 content on upconversion luminescence is compared with that of other factors and discussed, and the possible

*Project supported by the National Natural Science Foundation of China (Grant No 60207006).
†E-mail: shiqingxu75@hotmail.com

upconversion mechanisms are evaluated.

2. Experiments

The glasses were synthesized by a conventional melt quenching method. The starting materials were reagent grade GeO_2, PbO and PbF_2. The compositions of the prepared glasses were $50GeO_2 - (50 - x)$ $PbO{-}xPbF_2$ (x=0, 10, 20, 30, 40, 50 in mol%). Er^{3+} was introduced as Er_2O_3 with 4N purity. The Er^{3+} doping concentration in the glasses was 1.0 mol%. Samples were named as in Table 1 to recognize the compositions easily. Batches, each about 50g of starting materials, were fully mixed and then melted between 900° and 1000° in covered silicate crucibles in a SiC Globar furnace in a N_2 atmosphere. When melting was completed, the glass liquids were cast onto stainless steel plates. The obtained glass samples were then cooled to room temperature at a rate of 10°/h, and was cut and polished carefully in order to meet the requirements for optical measurements. Undoped GPF0 and GP50 glasses were also prepared for measuring the vibrational spectra.

Table 1. T_x, T_g and $\Delta T = T_x - T_g$ of Er^{3+}-doped $50GeO_2 - (50 - x)$ $PbO{-}xPbF_2$ (x=0, 10, 20, 30, 40, 50 in mol%) glasses.

Glass samples	x /(mol%)	T_x /(°)	T_g /(°)	$\Delta T = T_x - T_g$ /(°)
GPF0	0	374	484	110
GPF10	10	344	470	126
GPF20	20	331	462	131
GPF30	30	320	457	137
GPF40	40	311	450	139
GPF50	50	302	447	145

The glass transition temperature (T_g) and the crystallization onset temperature (T_x) were determined by differential thermal analysis (DTA) at a heating rate of 10°/min, using aluminium oxide ceramic pan. UV/VIS/NIR absorption spectra were recorded between 250 and 1700nm using a spectrophotometer on 2 mm thick glass samples optically polished. The upconversion luminescence spectra were obtained with a TRIAX550 spectrofluorimeter upon excitation of 975 nm laser diode (LD) with a maximum power of 2W. In order to compare the luminescence intensity of Er^{3+} in different samples as accurately as we can, the position and power (100 mW) of the pumping beam and the width (1 mm) of the slit to collect the luminescence signal were fixed under the same condition, and the samples were set at the same place in the experimental setup. In addition, the integrated intensities for the green and red emissions were also calculated to illustrate the variation of the luminescence intensity. Raman spectrum was recorded on a Fourier transform Raman spectrophotometer (Nicolet MODULE) within the range of 100–1200cm^{-1}. Nd: YAG laser operating at 1064 nm was used as the excitation source, and the laser power level was 500 mW. All the measurements were carried out at room temperature.

3. Results and discussion

A typical DTA curve of Er^{3+}-doped GPF50 glass is illustrated in Fig.1 in which the glass transition temperature (T_g) and the crystallization onset temperature (T_x) are marked. The difference between T_x and T_g, $\Delta T = T_x - T_g$, is used as usual as a rough estimate of the glass formation ability or glass stability. Since fibre drawing is a reheating process and any crystallization during the process will increase the scattering loss of the fibre and then degrade its optical properties.[13] To achieve a large temperature range during the sample fibre drawing, it is desirable for a glass host to have ΔT as large as possible.[13,14] Table 1 shows the compositional dependence of T_x, T_g, and $\Delta T = T_x - T_g$ of Er^{3+}-doped $50GeO_2 - (50 - x)$ $PbO{-}xPbF_2$ (x=0, 10, 20, 30, 40, 50 in mol%) glasses. With increasing content of PbF_2, T_x and T_g decrease, while $\Delta T = T_x - T_g$ increases. From Table 1, it can be seen that the ΔT value of all Er^{3+}-doped new heavy metal oxyfluoride germanate glasses is larger than 100°, indicating that these glass samples are very stable against devitrification.[15] The introduction of PbF_2 leads to a decrease of T_x, and T_g of these glass samples. Such a feature can be explained as follows: with the substitution of PbF_2 for PbO, owing to the gradual replacement of the Pb=O double bonds by two Pb–F single bonds, the structure of glasses becomes looser, thus the network structure is weakened, and the T_x and T_g of the glass samples are decreased. The ΔT value of these glass samples will increase because T_g is decreased more quickly than T_x.

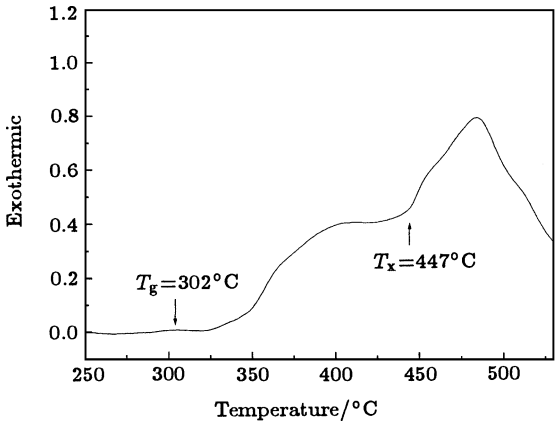


Fig.1. The DTA curve of Er^{3+}-doped GPF50 glass.

Figure 2 shows the Raman spectra of undoped GPF0 and GPF50 glasses. For GPF50 glass, three Raman bands around 376, 523 and 793 cm^{-1} originating from the Pb–F, Ge–O^- and O–Ge–O vibrational bonds, respectively, are observed. However, two Raman bands around 820 and 553 cm^{-1} for GPF0 glass originating from the Ge–O^- and O–Ge–O vibrational bonds, respectively, are observed. Compared with pure GeO_2 glass,[16] the peaks of Ge–O^- and O–Ge–O vibrational bonds are shifted to long wavelength, and the effect of PbF_2 on the peaks of Ge–O^- and O–Ge–O vibrational bonds is greater than that of PbO. Such features can be explained as follows: the intensities of Ge–O^- and O–Ge–O vibrational bonds are weakened due to the polarization of Pb^{2+} and the fluoride ions with lower phonon energy added into the glass network.[17] The spectrum indicates that the highest-frequency phonon band for GPF50 glass is at 793 cm^{-1}, smaller than that of pure GeO_2 glass which has a maximum phonon band at 865 cm^{-1}.[16] The highest-frequency phonon band of glass hosts is

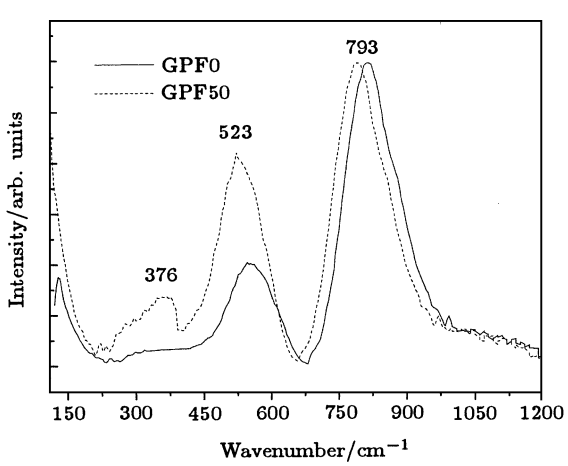


Fig.2. The room-temperature Raman spectrum of undoped GPF0 and GPF50 glasses.

critical for determining the upconversion efficiency. The lower phonon energies of heavy metal oxyfluoride germanate glasses can reduce the multiphonon loss, enhance radiative transitions of Er^{3+} and thus realize strong upconversion.

Figure 3 shows the absorption spectra of Er^{3+}-doped GPF0, GPF20 and GPF50 glasses. Each assignment corresponds to an excited level of Er^{3+}. The absorption spectrum consists of 11 absorption-band peaks at 1532, 975, 801, 651, 542, 521, 487, 450, 442, 406, and 378 nm, corresponding to the absorptions from the ground state $^4I_{15/2}$ to the excited states $^4I_{13/2}$, $^4I_{11/2}$, $^4I_{9/2}$, $^4F_{9/2}$, $^4S_{3/2}$, $^4H_{11/2}$, $^4F_{7/2}$, $^4F_{5/2}$, $^4F_{3/2}$, $^2H_{9/2}$, $^4G_{11/2}$, respectively. The wavelengths of the absorption peaks scarcely change with increasing content of PbF_2, but the cut-off band is shifted from 370 to 290 nm. Owing to the potential (4.03 eV) of F^- being greater than the potential (3.80 eV) of O^{2-}, the forbidden band gap of the glass is broadened as a result of doping F^- into oxide glasses network, and the transition of electrons from valence band to conduction band needs much bigger energy, and thus the cut-off band is shifted to shorter wavelength. It was also observed that the amplitude of the band near 800 nm is lower than that near 975 nm, which indicates that Er^{3+} in heavy metal oxyfluoride germanate glasses can be excited effectively by 975 nm LD.

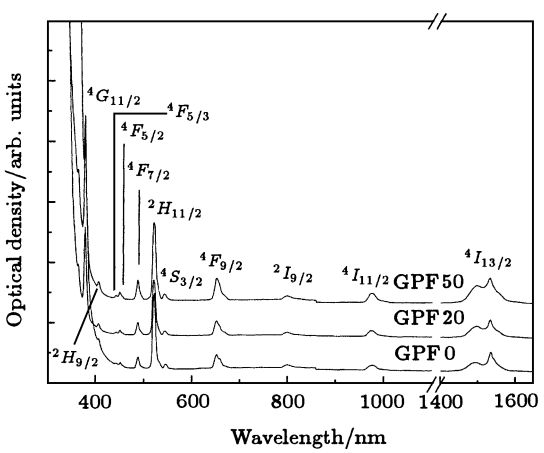


Fig.3. The absorption spectra of Er^{3+}-doped GPF0, GPF20 and GPF50 glasses.

The room-temperature upconversion luminescence spectra of Er^{3+} in heavy metal oxyfluoride germanate glasses with different PbF_2 contents excited by a 975 nm LD are shown in Fig.4. Three emission bands centred at 529, 551, and 657 nm, which correspond to the transitions $^2H_{11/2} \rightarrow^4 I_{15/2}$, $^4S_{3/2} \rightarrow^4 I_{15/2}$, and $^4F_{9/2} \rightarrow^4 I_{15/2}$, respectively, are simultane-

ously observed. It is also important to point out that the green emission is bright enough to be observed by naked eye at excitation power as low as 60 mW for Er^{3+}-doped GPF50 glass sample. Figure 5 illustrates the dependence of upconversion luminescence intensity on PbF_2 content. With increasing content of PbF_2, the intensities of green (529 nm) and red (657 nm) emissions increase slightly, while the green emission increases greatly. The relative intensity of green (551 nm) emission in Er^{3+}-doped GPF50 glass increases by a factor of 141.2 as compared with that in Er^{3+}-doped GPF0 glass. These results suggest that PbF_2 has stronger influence on the green (551 nm) emission than on the green (529 nm) and red (657 nm) emissions.

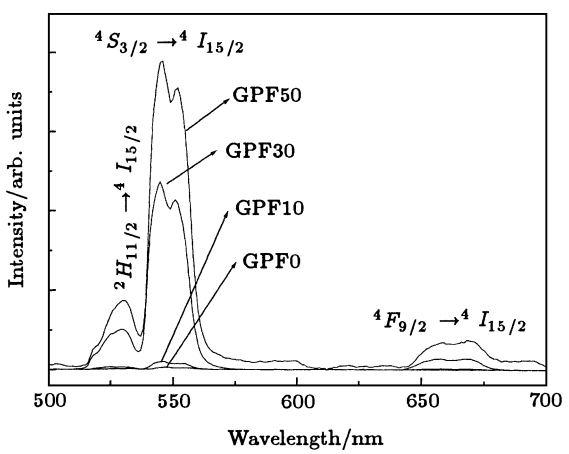


Fig.4. Upconversion luminescence spectra of Er^{3+}-doped GPF0, GPF10, GPF30, and GPF50 glasses under 975 nm excitation at room temperature.

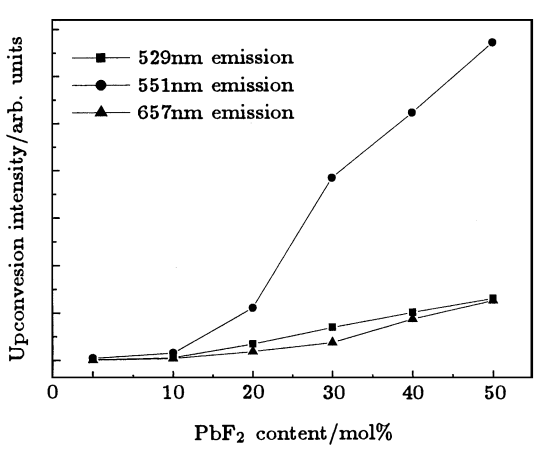


Fig.5. Upconversion luminescence intensities of Er^{3+}-doped $50GeO_2 - (50 - x)$ $PbO - xPbF_2$ glasses (x=0, 10, 20, 30, 40, 50 in mol%).

The power dependence of the aforementioned upconversion signals has been also analysed and the results are depicted in log–log plots of Fig.6. As can be seen, all the three emissions present quadratic dependence on the excitation power, which indicates that two photon steps are involved for the upconversion process.[3] According to the energy matching conditions and the quadratic dependence on excitation power, the possible upconversion mechanisms for the emission bands are discussed based on the simplified energy levels of Er^{3+} presented in Fig.7.[18–20] For the green emissions, in the first step, the $^4I_{11/2}$ level is directly excited at 975 nm. The second step involves the excitation processes based on the long-lived $^4I_{11/2}$ level as follows: energy transfer (ET) $^4I_{11/2}$ (Er^{3+}) $+{}^4I_{11/2}$ (Er^{3+}) $\rightarrow{}^4F_{7/2}$ (Er^{3+}) $+{}^4I_{15/2}$ (Er^{3+}), and excited state absorption (ESA) $^4I_{11/2}$ (Er^{3+})+a photon $\rightarrow{}^4F_{7/2}$ (Er^{3+}). The populated Er^{3+} $^4F_{7/2}$ level then relaxes rapidly and nonradiatively to the next lower levels $^2H_{11/2}$ and $^4S_{3/2}$, resulting from the small energy gap between them. It is considered that the $^2H_{11/2}$ level is populated from $^4S_{3/2}$ by a fast thermal equilibrium between the levels.[21,22] The above processes then produces the two $^2H_{11/2} \rightarrow{}^4I_{15/2}$ and $^4S_{3/2} \rightarrow{}^4I_{15/2}$ green emissions centred at 529 and 551 nm, respectively. Since the energy gap below the $^4S_{3/2}$ level is larger, for example, over 3100 cm^{-1}, obtained from the absorption spectrum data of Er^{3+}-doped GPF50 glass, the nonradiative transition through mutiphonon relaxation from $^4S_{3/2}$ level becomes smaller. Therefore, the bright green upconversion luminescence was emitted through the $^4S_{3/2} + {}^2H_{11/2} \rightarrow{}^4I_{15/2}$ transitions. The relatively weak red emission centred at 657 nm originates from the $^4F_{9/2} \rightarrow{}^4I_{15/2}$ transition. The population of $^4F_{9/2}$ are based on the processes as follows: ESA: $^4I_{13/2}$ (Er^{3+})+a photon $\rightarrow{}^4F_{9/2}$ (Er^{3+}), and ET between Er^{3+} ions: $^4I_{13/2}$ (Er^{3+}) $+{}^4I_{11/2}$ (Er^{3+}) $\rightarrow{}^4I_{15/2}$ (Er^{3+}) $+{}^4F_{9/2}$(Er^{3+}). The $^4I_{13/2}$ level is populated due to the nonradiative relaxation from the upper $^4I_{11/2}$ level. Besides, the nonradiative process from the $^4S_{3/2}$ level, which is populated by means of the process described previously, to $^4F_{9/2}$ level also contributes to the red emission.

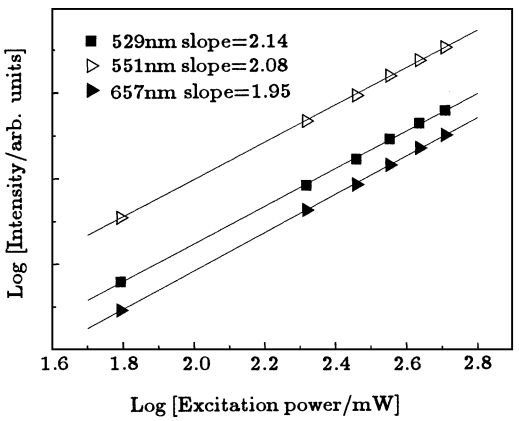


Fig.6. Dependence of upconversion fluorescence intensity on excitation power under 975 nm excitation for Er^{3+}-doped GPF50 glass.

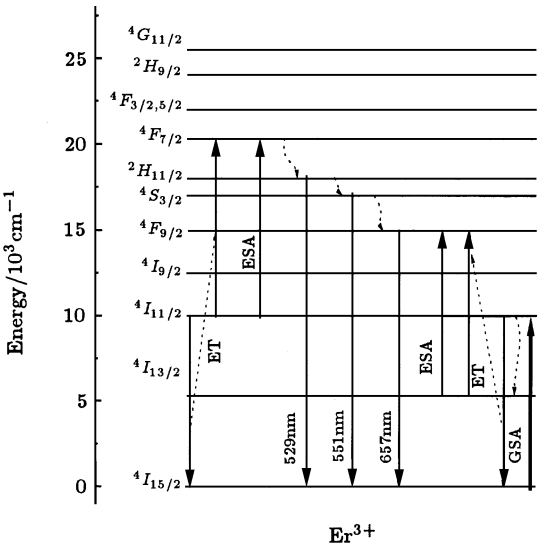


Fig.7. Energy level of Er^{3+} and possible transition pathways in Er^{3+} doped heavy metal oxyfluoride germanate glass.

4. Conclusion

We have demonstrated an efficient infrared to visible upconversion system of Er^{3+}-doped heavy metal oxyfluoride germanate glasses. Under 975 nm excitation, intense green (551 and 529 nm) and relatively weak red (657 nm) emissions are observed at room temperature. The upconversion processes involve a sequential two-photon absorption for the green and red emission. With increasing content of PbF_2, T_x and T_g decrease, while $\Delta T = T_x - T_g$ increases, and the intensities of green (529 nm) and red (657 nm) emissions increase slightly, while the green emission (551 nm) increases markedly. The relative intensity of green (551 nm) emission in Er^{3+}-doped GPF50 glass increases by a factor of 141.2 as compared with that in Er^{3+}-doped GPF0 glass. Intense green upconversion luminescence of Er^{3+}-doped GPF50 glass can serve as potential materials for developing upconversion optical devices.

References

[1] Man S O, Pun E Y B and Chung P S 2000 *Appl. Phys. Lett.* **77** 483

[2] Xu S Q, Wang G N and Zhang J J 2004 *Acta Phys. Sin.* **53** 1840 (in Chinese)

[3] Fen X, Chen X B and Hao Z 1997 *Acta Phys. Sin.* **46** 2454 (in Chinese)

[4] Higuchi H, Takahashi M and Kawamoto Y 1998 *J. Appl. Phys.* **38** 19

[5] Xu S Q, Yang Z M and Zhang J J 2004 *Chem. Phys. Lett.* **385** 263

[6] Murata T, Moriyama Y and Morinaga K 2003 *Sci. Technol. Adv. Mater.* **1** 139

[7] Xu S Q, Yang Z M and Dai S X 2003 *Chin. Phys.* **12** 997

[8] Lin H, Pun E Y B and Man S Q 2001 *J. Opt. Soc. Am.* B **18** 602

[9] Porque J, Jiang S B and Hwang B C 2000 *Proc. SPIE* **3942** 60

[10] Yamada H and Kojima K 1999 *J. Non-Cryst. Solids* **259** 57

[11] Kojima K, Fujita T and Yamazaki M 1999 *J. Non-Cryst. Solids* **259** 63

[12] Xu S Q, Yang Z M and Wang G N 2004 *Spectrochim. Acta* Part A **60** 3025

[13] Neindre L L, Jiang S B and Hwang B C 1999 *J. Non-Cryst. Solids.* **255** 97

[14] Drexhage M G, Bayoumi O H and Moyniyan C T 1982 *J. Amer. Ceram. Soc.* **65** 168

[15] Wang J S, Vogel E M and Snitzer E 1994 *J. Non-Cryst. Solids* **178** 109

[16] Pan Z, Morgan S H and Loper A 1995 *J. Appl. Phys.* **77** 4688

[17] Xu S Q, Wang G N and Zhang J J 2004 *J. Non-Cryst. Solids* **336** 230

[18] Auzel F 1990 *J. Lumin.* **45** 341

[19] Joubert M F 1999 *Opt. Mater.* **11** 181

[20] Lin H, Meredith G and Jiang S 2003 *J. Appl. Phys.* **93** 186

[21] Maurice E, Monnom G and Dussardier B 1995 *Opt. Lett.* **19** 990

[22] Berthou H and Jorgensen C K 1990 *Opt. Lett.* **15** 1100